# COMPARISON BETWEEN EULERIAN-EULERIAN NUMERICAL SIMULATION AND EXPERIMENTS ON SINGLE NARROW CHANNEL MIXTURE FLOW

A Thesis

by

SANG-YEON CHOI

Submitted to the Office of Graduate and Professional Studies of
Texas A&M University
in partial fulfillment of the requirements for the degree of

MASTER OF SCIENCE

| | |
|---|---|
| Chair of Committee, | Kumbakonam Rajagopal |
| Committee Members, | Kan Wu |
| | Timothy Jacobs |
| Intercollegiate Faculty Chair, | Timothy Jacobs |

August 2019

Major Subject: Interdisciplinary Engineering

# ABSTRACT

Currently, many engineering challenges addressing the flow of mixtures exist. Slickwater hydraulic fracturing is an economical method of unconventional resource extraction that can accelerate mixture flow. For this thesis, the flow of a sand-water mixture and its dune shape were observed. The aim of this study is to investigate similarities between simulated and experimental results by comparing peak height and volume ratios.

The flow described above is also called a "proppant flow" or "frac sand flow", one of the ways of enhancing shale gas production. After horizontal drilling, solid material is used to keep an induced hydraulic fracture open. The permeability of a proppant with cracks developed during production can endure high closure stress by the mantle. An example of this was expressed by the following experiment and simulation of the study.

An experimental study was conducted by a single narrow channel with the flow of a mixture. Particle size and volume injection rate are the main parameters that we controlled. Sand concentration as well as density were restricted for the experiment. Also, the total particle number and inlet speed of the mixture for the simulation were calculated with certain parameters.

Among numerous models, the standard K-$\varepsilon$ turbulence model was employed as a tool for analyzing solid and fluid materials for this task. We tried to verify the accuracy of these Eulerian-Eulerian methods by comparing the sand particle's diffusion and deposition results between a simulation and experiment. Comparison of both results was conducted by a post image processing tool on each step, time by time.

The study contains specific cases of hydraulic fracturing, and with this, validation of the turbulence model simulation accuracy is one of the aims. The comparison of each result is not only important regarding cost and time saving aspects, but also in showing that a simulation of each case is more efficient than time by time experiments.

DEDICATION

I can dim the lights and sing a songs full of sad things,

We can do the Tango just for two,

I can serenade and gently play for your heart strings,

Be a Valentino just for you.

Let me feel your heart beat,

Can you feel my love heat?

Come on and sit on my hot seat of love and tell me how do you feel right after all

I'd like for you and I to go romancing,

***"Say the word, your wish is my command."***

- Good old fashioned lover boy, Freddie Mercury

# ACKNOWLEDGMENTS

I've met so many thankful people during my two years of studying.

First of all, I want to say my love to my parents. They've given me this exciting life and still, they are giving all of them. I can't find any good words to express my mind.

Professor Rajagopal, one of the giants who make me available to see far, the greatest mentor gave me a chance to see what is a deep scientific critical thinking. The view I obtained from him is an invaluable worth of my entire life. I wish his healthy and happy life forever.

I want to give a special thanks for friends, tentative doctor Tejasvi Krishna Khambamphati, Dr. Hisasi Tani and his wife Haruko Tani. Their warmness was good energy for me to endure the College Station life. It was a short time to know each other, but I believe we will keep our relationship for a long long time. I hope these friends' happiness ever and after.

Manoj Myneni, Bhaskar Vajipeyajula, Akshay Rao, Dr. Juan Pablo, Pavitra Tejaswi, the friends who I met in TAMU from 2017 to 2019 gave me also good memory to remember this Texas life.

I remember my best friend, Elizabeth Lee. I want to give a big appreciation to her. Even though also she was a newcomer of Texas, but I've got a lot of advice and care from her. I will never forget this kindness ever.

# CONTRIBUTORS AND FUNDING SOURCES

## Contributors

The study has been supported by a Dr. Kumbakonam Rajagopal, Dr. Timothy Jacobs of the Department of the Mechanical Engineering and Dr. Kan Wu of the Department of Petroleum Engineering. All of the experimental data was obtained by Dr. Wu's laboratory experiment works, which is especially done by S.H. Chun, the Ph. D student of Dr. Wu.

The analyses depicted in Chapter II were conducted by Dr. Rajagopal of the Department of Mechanical engineering and were published in (1991) in an article listed in the Chemical Engineering Science Vol.46. All of the experiment condition for Chapter III was provided by Professor Wu and her Ph. D Student, Chun. As well as the experiment was conducted in their Department of Petroleum Engineering experiment laboratory.

I really appreciate their help in this study.

## Funding Sources

There are no outside funding contributions to acknowledge related to the research and compilation of this document.

# NOMENCLATURE

| | |
|---|---|
| NSE | Navier-Stokes Equation |
| CFD | Computational Fluid Dynamics |
| EE | Eulerian-Eulerian |
| LE | Lagrangian-Eulerian |
| RANS | Reynolds Averaging of the Navier-Stokes |
| DEM | Discrete Element Method |
| API | American Petroleum Institute |
| ISO | International Organization for Standardization |
| ASTM | American Society for Testing and Materials |
| EA | Each |
| GPM | Gallon Per Minute |
| PPG | Pound Per Gallon (1 pound per US Gallon = 119.826427 kg/$m^3$ |

TABLE OF CONTENTS

Page

LIST OF FIGURES

FIGURE Page

# LIST OF TABLES

TABLE Page

# 1. INTRODUCTION

A lot of descriptions of mixtures are in the world, but one of the definitions in a dictionary was most impressive: "A substance containing two or more ingredients, but this is totally different from a chemical compound, it does not lose their individual characteristics, and can be separated by physical means" [2]. Other authors defined mixture as "A composition of two or more substances that are not chemically combined with each other and are capable of being separated". Following the definition, there are uncountable numbers of mixtures existing in the world, many which are ubiquitous. The point of these explanations is the meaning "physically mixed matter by multiple components". In this study, we will consider a solid-fluid mixture which does not share the same phase and one which is not compounded.

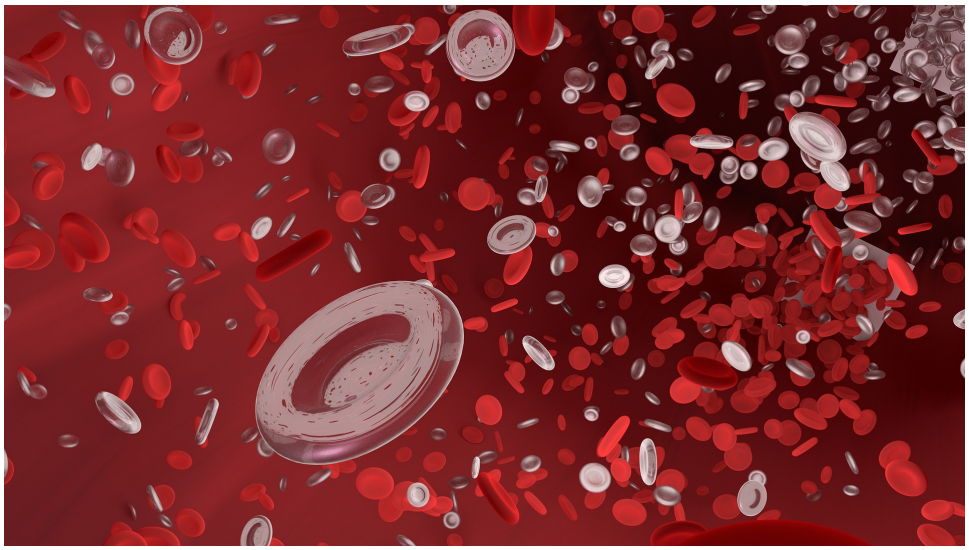

Figure 1.1: Blood mixture components, reprinted from pixabay.com

Not only are quite detailed verbal definitions of mixtures all around, but also flow of mixture streams has been greatly emphasized in numerous industrial and academic areas. Blood flow is an example that described in figure 1.1, and includes research carried out by J. Humphrey and

Rajagopal [3]. There are still many efforts to build an adequate model to address internal blood flow in the body.

Figure 1.2: Discharge of slurry, reprinted from [1]

Slurry pipeline flow is another good example of a mixture flow, figure 1.2 is one of good example. Two-phase flow in cylinder shape geometry was studied by D. H. Beggs et al.[4]. These types of scientific and industrial applications require cost-effective methodology studies concerning their mixture flow rates.

To analyze mixtures, we have to think about fluids first. From the beginning of fluid studies, a lot of analysis methods have been developed steadily and propagated to lots of academic areas. Fluid flow is one research field which has been intensively investigated by industrial engineering. These efforts started with the greatest scientists, Newton, Euler, Navier[4], Cauchy[5], Poisson, Saint-Venant, and so on. And finally, Stokes first used the absolute viscosity concepts[6]. Also, from the establishment of the Navier-Stokes equation, engineers and scientists have continuously dedicated their efforts to solving the equation with adequate assumptions. Nowadays, these dedications are specialized as a part of the academic branch, Computational Fluid Dynamics (CFD), which is one the most analytical ways of approaching the nearest solution of a partial differential equation. It has been developed by broad industrial and academic parts. Development of computer

hardware and improved calculation abilities have eased time and cost saving approaches in the CFD field.

Furthermore, there are a lot of endeavors of scientists and engineers for analyzing the flow of mixtures. Most of the general engineering areas like chemical and mechanical, ocean, even petroleum fields need these sorts of skillsets. Among them, this study will treat it as a branch of mixture study, a solid-fluid mixture flow.

The origin of mixture analysis started with Fick [5] and Darcy [6], two early pioneers who endeavored in the study of mixtures. These attempts have affected research of the diffusion of flow through other mixed media. One of it is the mixture theory which is proposed by Rajagopal and Tao[7]. Then, from a great improvement of computational hardware and software developments, numerical simulation accuracy has steadily evolved, thus these extraordinary speeds make it possible to compute numerous non-linear differential equations by relatively more accurate numerical approaches.

With the computational development back to the CFD in the modeling of the flow, generally two methods are used, the Eulerian and Lagrangian methods. The Eulerian method treats the particle phase as a continuous media and treats its conservation equations with a control volume basis and in a similar form as that for the fluid phase. This is one of a conventional method to study fluids. Moreover, it can be adjusted for granular materials with adequate assumptions.

Three general methods for analyzing this solid-fluid mixture are usually employed for the investigation, all which had been studied by K. Hutter et al[8]. The first is "Continuum mechanical approach" using balance relations of mass, momentum, and energy. The first is the "Continuum mechanical approach," using balanced relations of mass, momentum, and energy. Next are the Eulerian-Eulerian (EE) and Lagrangian-Eulerian (LE)[9] [10], which are usually approached by a fraction ratio of each base material. In this study, we will pay attention to the comparison of experimental data with the theoretical background performed by Eulerian-Eulerian simulations.

The work is motivated by petroleum engineering experimentation, "Hydraulic Slickwater Fracturing", which is a special petroleum well stimulation technique in which rock is fractured by a

pressurized solid and liquid mixture. Nowadays these well stimulating techniques are used broadly in shale-gas production areas. Already by the middle of the 20th century, some estimation of general fracturing area calculation techniques were proposed by George C. Howard et al[11]. Furthermore since that time, system research has continued, and many new skill sets have been developed. There are many variations of materials that are used in hydraulic fracturing work. However, in this study, a type of material will be used which is called a "Frac sand" or "Proppants"[12]. Specifically, the southern white frac sand type was used for the experiments. The result of some specific condition comparing which is done in this study will be also valuable for the efficiency of future research.

# 2. LITERATURE REVIEW

## 2.1 Summary of governing equations

Basically, the phenomenon that is treated in this paper is slurry flow, which is the transport motion of sand particles mixed with liquids. The volume fraction equations were used by G.Johnson et al. [13].

$$\rho_1 = \phi\rho_f, \quad \rho_2 = \nu\rho_s \tag{2.1}$$

Where the $\rho_f$ is the density of the pure fluid, and $\rho_s$ is the density of the solid. $\nu$ is the volume fraction of the solid component, and the $\phi$ is the volume fraction of the fluid. This can be described when the media is assumed as a fully saturated mixture.

$$\phi = 1 - \nu, \tag{2.2}$$

$$\rho_m = \rho_f + \rho_s \tag{2.3}$$

The overall mixture mean velocity $\mathbf{v}_m$ can be described as;

$$\rho_m \mathbf{v}_m = \rho_f \mathbf{v}_f + \rho_s \mathbf{v}_s \tag{2.4}$$

### 2.1.1 Conservation of mass

First of all, mass terms should be considered for the entire analysis. The volume-averaged, incompressible, isothermal, and transient for both phases are given by B. G. M. Van Wachem at el. [14] and Andersson, Bengt; et al. [15]. And, these equations are equivalent to below;

$$\frac{\partial}{\partial t}(\rho_f) + \nabla \cdot (\rho_f \mathbf{v_f}) = \mathbf{0} \tag{2.5}$$

$$\frac{\partial}{\partial t}(\rho_s) + \nabla \cdot (\rho_s \mathbf{v_s}) = \mathbf{0} \tag{2.6}$$

When we adjust the volume fraction to the term(2.5), we can obtain;

$$\frac{\partial \nu}{\partial t} = \nabla \cdot (\nu \mathbf{v_m}) \tag{2.7}$$

$$\frac{\partial \phi}{\partial t} = \nabla \cdot (\phi \mathbf{v_m}) \quad = \quad \frac{\partial (1-\nu)}{\partial t} = \nabla \cdot ((1-\nu)\mathbf{v_m}) \tag{2.8}$$

Some assumptions that interconversion of mass between of the two each component exists in the problem, but These terms are assumed there is no interconversion of mass between the two constituents.

### 2.1.2 Conservation of linear momentum

G. Johnson et al. [13] also denotes the linear momentum with,

$$\rho_f \frac{D\mathbf{v_f}}{\mathbf{Dt}} = \nabla \cdot \mathbf{T_f} + \rho_\mathbf{f} \mathbf{b_f} + \mathbf{f_I} \tag{2.9}$$

$$\rho_s \frac{D\mathbf{v_s}}{\mathbf{Dt}} = \nabla \cdot \mathbf{T_s} + \rho_\mathbf{s} \mathbf{b_s} - \mathbf{f_I} \tag{2.10}$$

Then $\mathbf{T_f}$ denote the partial stress tensors of fluid phase of the material, $\mathbf{T_s}$ is for the solid phase. Also, $\mathbf{b_f}$ and $\mathbf{b_s}$ represents the body force of each phase respectively, and $\mathbf{f_I}$ indicates the mechanical interaction between each component. Also, partial stress tensors can be denoted the relationship of each $\mathbf{T}$ by volume fraction,

$$\mathbf{T_f} = \phi \mathbf{T_s}, \quad \mathbf{T_s} = \nu \mathbf{T_f} \tag{2.11}$$

$m_i$ and $v_i$ are mass and velocity of particle i, $F_g$ is gravity force, thus $F_g = m_i g$, and $F_{ij}$ is the contact force between particle i and element j.

### 2.1.3 Conservation of angular momentum

By Massoudi et al.[16], the conservation of angular momentum is not needed to consider because the total stress tensor for the mixture is symmetric, though the partial stresses need not be

symmetric, even though the principle implies that;

$$\mathbf{T_1} + \mathbf{T_2} = \mathbf{T_1^T} + \mathbf{T_2^T} \tag{2.12}$$

## 2.2 Constitutive assumptions

To analyze mixture flow phenomenons, some assumptions must be considered and put in the simulations. Each condition has its own meaning in simulation, thus the conditions should be viewed and treated delicately. There are some assumptions based on fluid mechanics and should be applied for adequate analysis results. Details are as like below;

1. We assume that the solid phase material has ideal rigid solid properties. Thus, there aren't deformations in solid particles.

2. We will not consider thermal effects. This means that the sort of processes are isothermal at a constant. So, the conservation of energy will not be considered in this study.

3. We shall suppose that the fluid is incompressible, linearly viscous material.

4. Particles settled on the bed are stored as a simple unit cubic shape structure uniformly.

5. The frictional effects in the fluid due to the viscosity can be neglected.

## 2.3 Turbulence models

Even though we have good equations to explain some phenomena, we should still use specific models to describe real situations. There is no single turbulence model that can be allowed as being superior for all of kinds problems, thus specific models must be chosen per situation. The model depends on considerations of each model by theories or experiences. Additionally, economic de-liberations such as computational resources or available time for the simulation should be also considered in industrial engineering. In other words, a practical number of nodes, adequate assumptions, and any other consideration points are absolute factors for analysis using turbulence models for more accurate approximations. Only after considering conditions and finding an adequate model by comparing and analyzing procedures, will the simulation will be carried out. Regarding hydraulics, W. Rodi et al. [17] mentioned examples of each model's real usage.

If it is possible, we can use Direct Numerical Solution which is also called DNS. However, this is generally too expensive for general engineering work. Therefore, some kinds of new models have been derived. Generally, many turbulence models had been established to analyze flow, and mentioned are brief overviews of some of the ones that are that commonly used in engineering applications. Common are linear eddy viscosity turbulence models obtained from Reynolds Averaging of the Navier-Stokes (RANS) equations. With a macro view, turbulence models can be divided into three types: the Algebraic model, one equation model, and two equation model[18].

Algebraic models are usually called Zero-equation models that do not require the solution of any additional equations. The calculation is conducted directly from flow variables; thus it is not influenced by convection, diffusion, or turbulent energy. There are some types of the one equation model. The Spalart-Allmaras model is a famous models of this category[19]. The model solves a transport equation for the kinematic eddy turbulent viscosity. This model was designed for aerospace wall-bounded flows which are subjected to adverse pressure gradients.

The Two equation model is one of the most common types of turbulence models in industrial realms because of its balance between accuracy and resource cost[20]. The most often transported variable in this consideration is turbulent kinetic energy, and as a consideration, the transported variable depends on the type of model. If we choose the $K - \varepsilon$ model, the turbulent dissipation $\varepsilon$ would be chosen, and when the $K - \omega$ model is picked, the specific turbulence dissipation rate $\omega$ would be used. There are many choices of a models that can be used in analysis, but the usage will depend on each situation and condition.

### 2.4 K-$\varepsilon$ model

For more than fifty years, two-equation turbulence models have been used analysis. Many models have been developed, and most of these models solve a transport equation for k, which is turbulent kinetic energy. The second transport equation makes it possible to consider a turbulent length scale to be defined. In the $K - \varepsilon$ model, the second transport term usually computes a $\varepsilon$, which means turbulent dissipation. In other words, turbulent kinetic energy $K$ which roughly describes the intensity of the turbulent motion, and the $\varepsilon$, the turbulent dissipation rate denotes the

length scale of the motion which is most commonly used[21].

The $K-\varepsilon$ model solves for two variables as mentioned before. This model has been very popular for industry due to its good convergence rate, relatively required low time, and cost values. Two equation gives a general description of turbulence by means of two transport equations. Various models like the Realisable model, RNG model, are in use even today, but in this thesis, the "Standard $K-\varepsilon$ model" will be used. The transport equations for the turbulent kinetic energy $K$ and dissipation $\varepsilon$ are as the following;

$$\frac{\partial(\rho k)}{\partial t}+\frac{\partial(\rho k \mathbf{u_i})}{\partial \mathbf{x_i}}=\frac{\partial}{\mathbf{x_j}}\left[\frac{\mu_t}{\sigma_\mathbf{k}}\frac{\partial k}{\partial \mathbf{x_j}}\right]+2\mu_t E_{ij}E_{ij}-\rho\varepsilon \tag{2.13}$$

$$\frac{\partial(\rho \varepsilon)}{\partial t}+\frac{\partial(\rho \varepsilon \mathbf{u_i})}{\partial \mathbf{x_i}}=\frac{\partial}{\mathbf{x_j}}\left[\frac{\mu_t}{\sigma_\varepsilon}\frac{\partial \varepsilon}{\partial \mathbf{x_j}}\right]+C_{1\varepsilon}\frac{\varepsilon}{k}2\mu_t E_{ij}E_{ij}-C_{2\varepsilon}\rho\frac{\varepsilon^2}{k} \tag{2.14}$$

The terms can be described "rate of change of $K$ or $\varepsilon$ + Transport of $K$ or $\varepsilon$ by convection = Transport of $K$ or $\varepsilon$ by diffusion + rate of production of $K$ or $\varepsilon$ - rate of destruction of $K$ or $\varepsilon$ ". $u_i$ represents velocity component in corresponding direction, $E_{ij}$ represents component of rate of deformation. $\mu_t$ is the value of $\rho C_\mu \frac{k^2}{\varepsilon}$. The equations also consist of some adjustable constants $\sigma_k$, $\sigma_\varepsilon$, $C_{1\varepsilon}$, and $C_{2\varepsilon}$. The values of these constants have been arrived at by numerous iterations of data fitting for a wide range of turbulent flows. The moderate values had suggested by BE Launder et al.[18] These are as follows;

$$C_\mu=0.09, \quad \sigma_k=1.00, \quad \sigma_\varepsilon=1.30, \quad C_{1\varepsilon}=1.44, \quad C_{2\varepsilon}=1.92 \tag{2.15}$$

# 3. MATERIALS AND METHODS

## 3.1 Properties and conditions

Results of the experiment and simulation are compared, and the displacement of the dune over their time steps will be discussed in section 4. Before the discussion, we have to identify the material properties and conditions of work.

Firstly, discussing properties of the sand and water which are used in the experiments should be conducted. These material properties are also put in the simulation data with appropriate assumptions. In the experiment, we used the "Frac sand", also called "Proppants", which is used in petroleum "Hydraulic Fracturing." Hereby documentation from API, ISO, ASTM and so on, regarding sand particle size have been already clearly regulated [22]. There are many types of sand for hydraulic fracturing, but in this case, "Southern white sand" which is one kind of frac sand proppant. In this experiment, we used three types of sands. The sand size table from the world oil proppant size publication was used for this study's information[23], the configuration is expressed below figure 3.1.

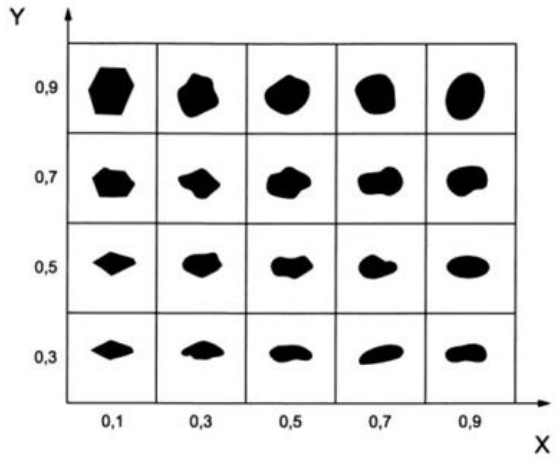


Figure 3.1: Chart for visual estimation of sphericity and roundness of sand particle

Sand sizes and shapes show variation when compared with each other. In this study, sand sizes and shapes are assumed to be homogeneous. Thus, averaged sand size would be taken for the property. As well, particle shapes were considered as a regular spherical forms. Also, there is one more assumption when the sands are laid on the bed, as each particle is piled as a simple cubic unit structure. This assumption is being used on the calculation of total particle numbers with sand density and inlet quantities of the mixture. The calculation charts are denoted in Figure 3.2. Then, the EE simulation model simulation result would be compared with experimental data. The data used in the experiment and simulation briefly calculated and suggested as below table 3.1 and 3.2;

| | **Description** | **Size** |
|---|---|---|
| **Sand size** | 20/40 | 0.630 (mm) |
| | 30/50 | 0.415 (mm) |
| | 40/70 | 0.315 (mm) |

Table 3.1: Sand properties

| | |
|---|---|
| Sand concentration | 1.5 ppg (lb/gal) |
| Sand density | 2.55 g/cm$^3$ |
| Fluid viscosity | 1 cp (Pa $\cdot s$) |

Table 3.2: Base concentration / density / viscosity properties

Then we have to consider more conditions, which are the basis of the calculation for the quantities. Based on the calculation results, we can obtain such conditions that we can use in simulations. Conditions that considered in simulation are described on table 3.3. Total sand particle numbers are calculated by using sand density, quantities and concentration. Inlet speeds are computed by volume injection rate and the values are divided by three because the channel that we used in the experiment has three inlets. These calculated values were treated when simulations are carried out. The results are below;

| case | Particle type | Particle Dia [mm] | Particle number [EA] | Volume injection rate [GPM] | Inlet speed [m/s] |
|---|---|---|---|---|---|
| **1** | 20/40 | 0.63 | 5,336,376 | 4.5 | 0.978 |
| **2** | 20/40 | 0.63 | 5,336,376 | 6.0 | 1.304 |
| **3** | 30/50 | 0.415 | 18,665,311 | 4.5 | 0.978 |
| **4** | 30/50 | 0.415 | 18,665,311 | 6.0 | 1.304 |
| **5** | 40/70 | 0.315 | 42,683,007 | 4.5 | 0.978 |
| **6** | 40/70 | 0.315 | 42,683,007 | 6.0 | 1.304 |

Table 3.3: Calculated restriction conditions

The data sets were obtained by calculation with particle assumptions which are indicated in figure 3.2. Assumptions that considered for the simulation are fully round, rigid bodied, and uniformly sized particle proppant properties. The calculation of unit converting main averaged velocity of the mixture and particle number is based on the information of particle diameter volume injection rate which is firstly confirmed by the experiment conditions. Converting of USCS units to the SI unit is the starting point of the chart, and particles that stuck as like a simple unit cubic face would have regular number per unit volume. By this assumption, the number of whole particle numbers could be obtained. With time and volume injection rate consideration, the rough proppant particle number condition was also obtained.

| | | | | | | | |
|---|---|---|---|---|---|---|---|
| GPM(Vol) | 4.5 | Gallon / minute | | 1 Gal | = | 0.00378541 | m^3 |
| Transferred unit | 0.0170343450 | m^3 / min | | 1 in | = | 0.0254 | m |
| Transferred unit | 0.0002839058 | m^3 / s | | | | | |
| | | | | | | | |
| Inlet dia | 0.3 | in | 0.5 | | | | |
| Transferred unit | 0.00762 | m | 0.013 | | | | |
| Area | 9.677400E-05 | m^2 | | | | | |
| | | | | | | | |
| Velocity(GPM/area) | 2.934 | m/s | | | | | |
| V per hole | 0.978 | m/s | | 20/40 particle no | | 5,336,376 | EA |

| | | | | | | | |
|---|---|---|---|---|---|---|---|
| GPM(Vol) | 6 | Gallon / minute | | 1 Gal | = | 0.00378541 | m^3 |
| Transferred unit | 0.0227124600 | m^3 / min | | 1 in | = | 0.0254 | m |
| Transferred unit | 0.0003785410 | m^3 / s | | | | | |
| | | | | | | | |
| Inlet dia | 0.3 | in | 0.5 | | | | |
| Transferred unit | 0.00762 | m | 0.013 | | | | |
| Area | 9.677400E-05 | m^2 | | | | | |
| | | | | | | | |
| Velocity(GPM/area) | 3.912 | m/s | | | | | |
| V per hole | 1.304 | m/s | | 30/50 particle no | | 18,665,311 | EA |

| | | | | | | | |
|---|---|---|---|---|---|---|---|
| GPM(Vol) | 7.5 | Gallon / minute | | 1 Gal | = | 0.00378541 | m^3 |
| Transferred unit | 0.0283905750 | m^3 / min | | 1 in | = | 0.0254 | m |
| Transferred unit | 0.0004731763 | m^3 / s | | | | | |
| | | | | | | | |
| Inlet dia | 0.3 | in | 0.5 | | | | |
| Transferred unit | 0.00762 | m | 0.013 | | | | |
| Area | 9.677400E-05 | m^2 | | | | | |
| | | | | | | | |
| Velocity(GPM/area) | 4.889 | m/s | | | | | |
| V per hole | 1.630 | m/s | | 40/70 particle no | | 42,683,007 | EA |

Figure 3.2: Calculation sheet of Velocity and particle number

## 3.2 Lab experiments

### 3.2.1 Geometry and Modeling approaches

The experiment was done by the single narrow channel with mixing equipment (also known as agitator), a pump, and other equipment for measuring and maintaining. Each piece of equipment was set up for a sand mixture delivering inside of the channel to make a sand dune. Sand properties are denoted on table 3.1 to 3.3. For the fluid phase, regular tap water was used for the experiment

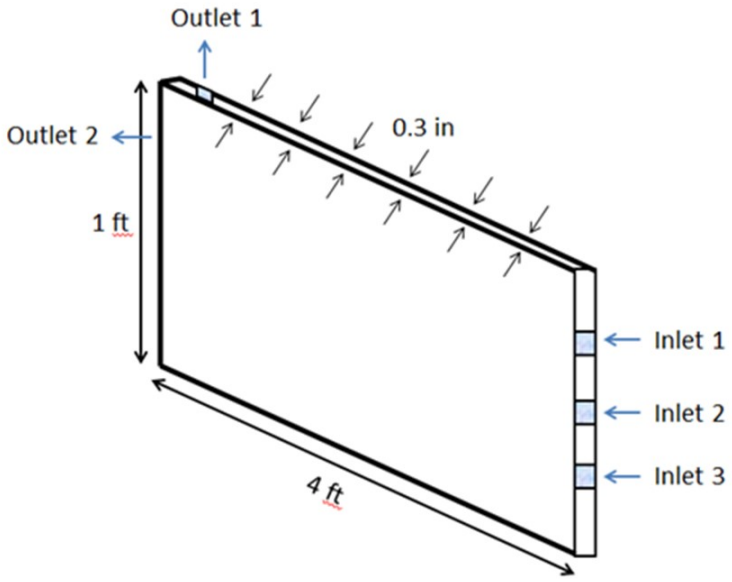


Figure 3.3: Dimensions of single channel used in experiment

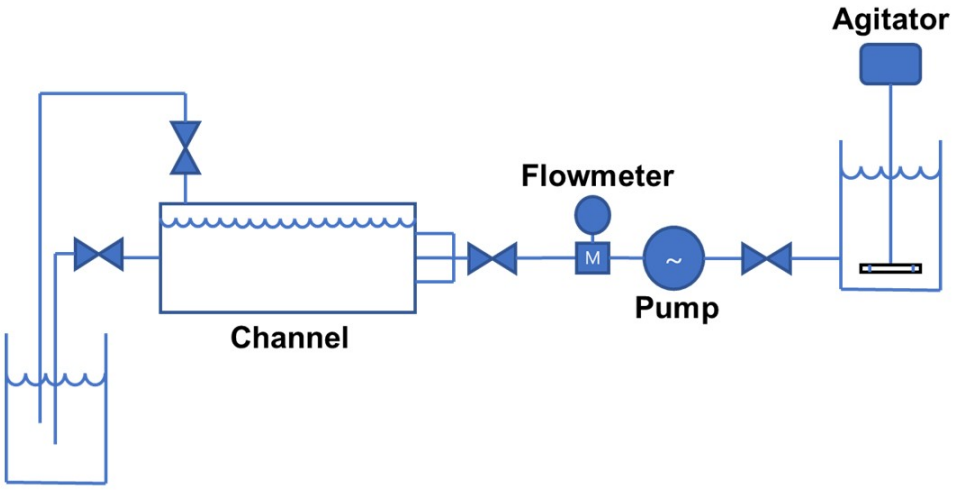


Figure 3.4: Overall experiment equipment configuration diagram

and it was assumed as 'pure water'. The single narrow channel was made by plexiglass panels. This channel is designed as four foot in length, one foot high, and 0.3 inches wide, looking like figure 3.2. There are three injection inlets on one side of the channel. Each hole has 0.3 inches by 0.5 inches of dimension. Nevertheless, inlet valves and hoses have a round shape, and 0.5 inches diameter dimension, but some assumptions that inlet hole shapes are square would be taken. Inlet holes are located at each three, six, and nine inches of height to those center points. Two of the outlets also have the same dimension of inlets, but one is located on another side of the inlets, and the other outlet was bored on the top, near the outlet side. The second outlet has nine inches of height at the center point from the bottom. The rough sketch of channel, experiment system configuration are suggested on Figure 3.3 and 3.4.

First, the channel condition had to be prepared which is fully filled with water. Before the mixture injection, the channel should be filled because we have to see the diffusion and accumulation of mixture in the fluid-filled condition. After these settings, the agitator would work with constant speed to make the sand-water mixture. It is assumed that the composition of the mixture is maintained regularly by the propelling of the agitator. After a few seconds of turning on the agitator, the slurry would be pumped to the channel directly. All of the input quantities are checked by the electric flowmeter that is installed next to the pump. Before the experiment, the exact flow of the planned quantity of the mixture is set manually with valve control. There are three inlet holes at the channel, thus the exact inlet flow rate of each hole will one third of initial flow rate from the agitator and pump. The channel will be filled with the sand and water after the experiment, the sand will form a dune curve. It would be grown continuously by each time step.

## 3.3 Simulations

### 3.3.1 Turbulence Model selection

Simulations were carried out with ANSYS FLUENT, one of the famous commercial codes in the industry. The adequate model that was chosen after the investigation was absolutely what we have to consider for simulations. In this case, the K-$\varepsilon$ model, which is referred to previously, would

be one of the tools for the analysis and it will be adjusted for both material flows.

In the study, the RANS-Based turbulence models were chosen for the analysis. Linear eddy viscosity models were used because the linear constitutive relationship with mean flow condition is also one of the assumed points for the simulations. One model called $K$-$\varepsilon$ model, which is one of "two-equation-model". Two more extra equation is added for the solution, the term of turbulent kinetic energy $K$, and the turbulent dissipation $\varepsilon$ are the additional two variables[24]. Also for this study, the standard $K$-$\varepsilon$ model was adjusted for the simulation because in the case, the mean pressure gradients are relatively small, thus the researchers could obtain reasonable outputs[25].

### 3.3.2 Numerical solving condition and post processing

The boundary conditions are each defined case by case, and each case particle selection is calculated by weight and volume. For the numerical simulations, SIMPLE phase couple scheme was taken for the whole calculation, and first-order upwind, the implicit scheme, was used in the simulation. Measuring the result of displacement by each time step is a main comparison topic data of this paper. Solid particle distribution will be discussed with the displacement data. The ANSYS FLUENT has its own numerical simulation method, which is based on the mean value.

Flow inlet and exit are set like former experimental plexiglass geometry. A detail input parameters calculation sheet were suggested in figure 3.2. Velocity, mass and each turbulence parameters are considered for the simulations. The pressure is also one of the big consideration points for the simulation, thus, the simplified calculation flow chart would be as like below in figure 3.5;

Step by step, the calculations are going through each equation solving procedure. During the calculation, three momentum equations and one mass conservation term will be treated. Each mean-valued-variables, $K$, and $\varepsilon$ values calculations are iterated until the conversing of each solution. These swiped values are obtained by the first order upwind, a SIMPLE phase couple scheme that already referred above.

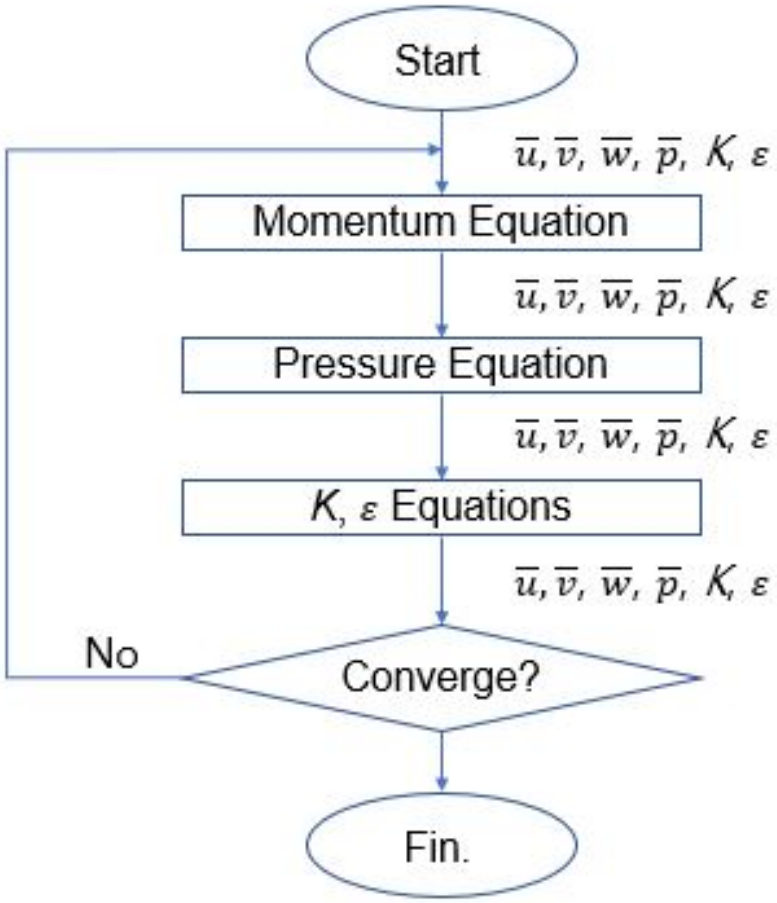


Figure 3.5: Brief flow chart of calculation procedure

# 4. SUMMARY AND DISCUSSION

## 4.1 Data summary

Between the plain single narrow channel sand height an experiment result and simulation of sand distribution data are plotted in Figure 4.1, 4.2 and 4.3. Each distribution profile is measured each time by time.

Figure 4.1: Result of experiment

First of all, the experiment data could be obtained as like figure 4.1. The dune height data was captured timewise, step by step, and those tendency data were processed by image processing tools.

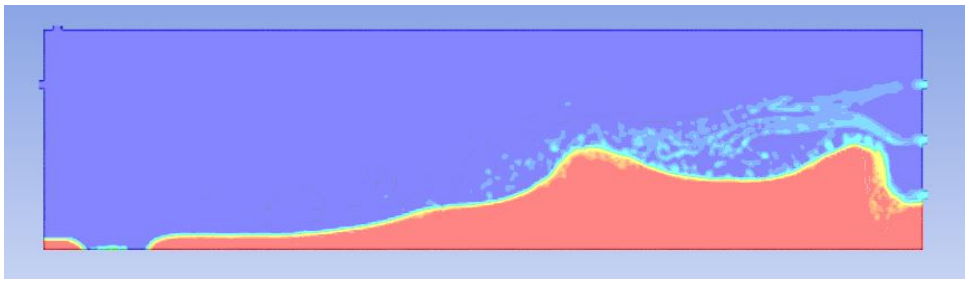

Figure 4.2: Result of Eulerian-Eulerian simulation

Simulation data sets were also captured each, time by time. Specific stepâĂŹs in time of dune

data were the basis of this analysis. More exact data could be obtained by color inverting.

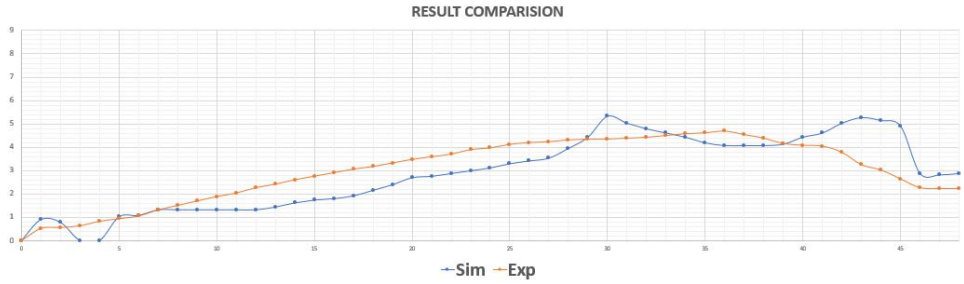


Figure 4.3: Result of Eulerian-Eulerian simulation post processing

After processing, result sets of simulation were expressed as like figure 4.3. The experimental conditions are mentioned in appendix A. At each inlet, the mixture has its own velocity, case by case. Experiment and simulation pictures were captured at twenty-five seconds from the beginning of each work. Exact data obtained by simulation and experiments were plotted by image processing.

Each experiment result was obtained by video recording and stopping at each time step. Also, the simulation results data were processed by time by time steps. In this thesis, the length and height of the sand dune were measured by image processing. Sections were divided by each 0.2 inches in height, and 1/6 inches in length. Above results are experimental samples to show the procedure briefly. Detailed results are suggested from figure 4.4 to figure 4.10;

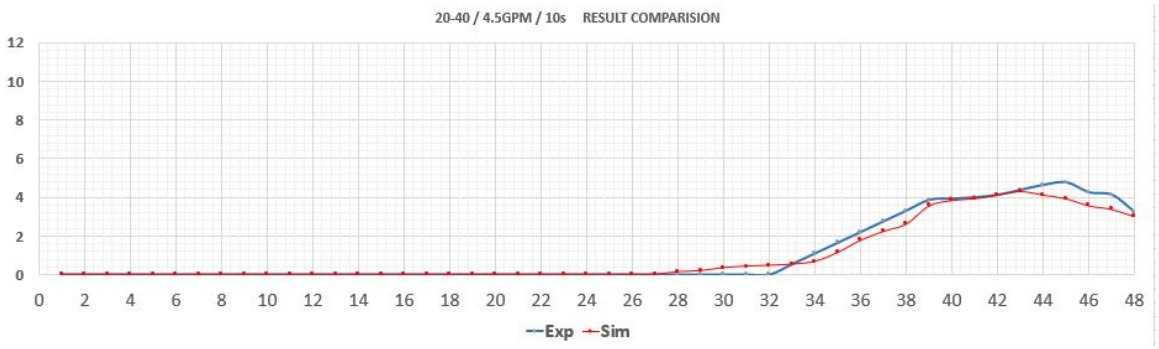


Figure 4.4: 20-40 Mesh / 4.5PPG / 10s

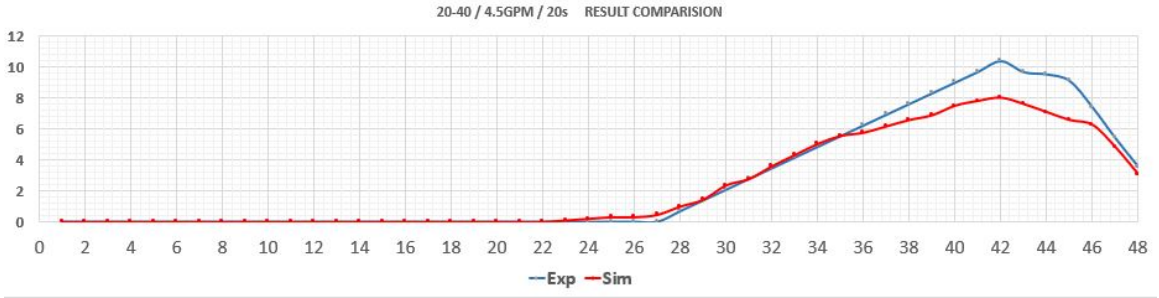


Figure 4.5: 20-40 Mesh / 4.5PPG / 20s

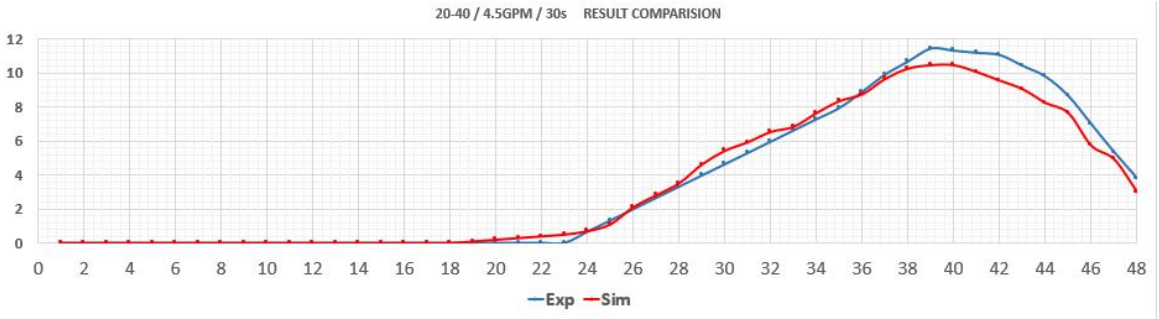


Figure 4.6: 20-40 Mesh / 4.5PPG / 30s

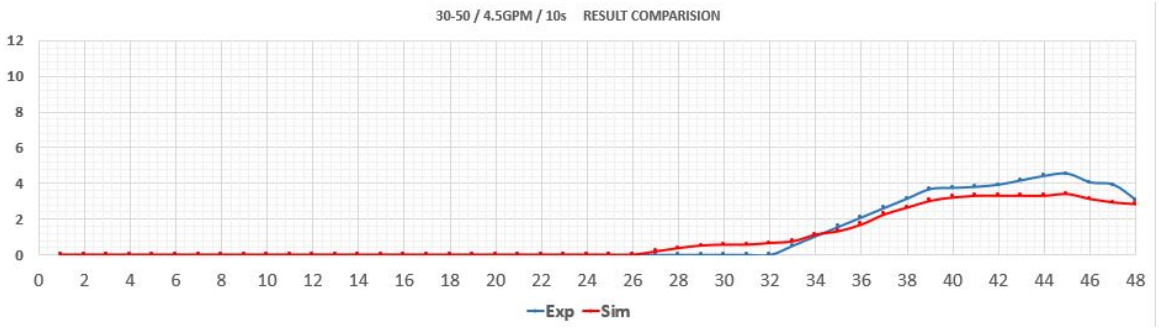


Figure 4.7: 30-50 Mesh / 4.5PPG / 10s

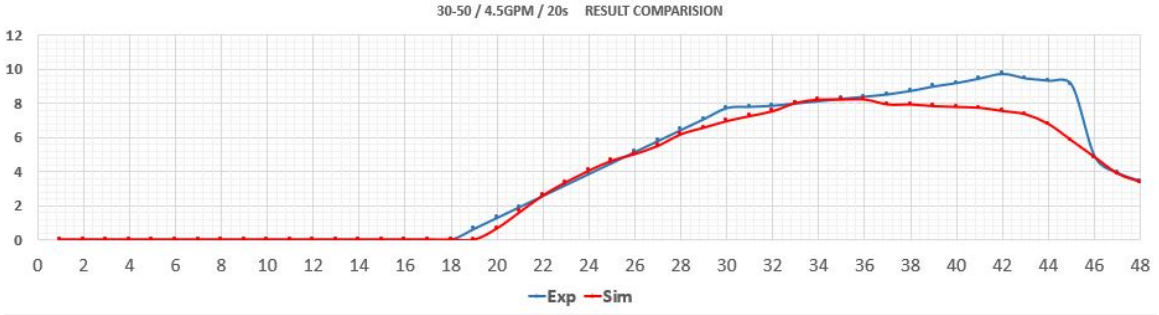


Figure 4.8: 30-50 Mesh / 4.5PPG / 20s

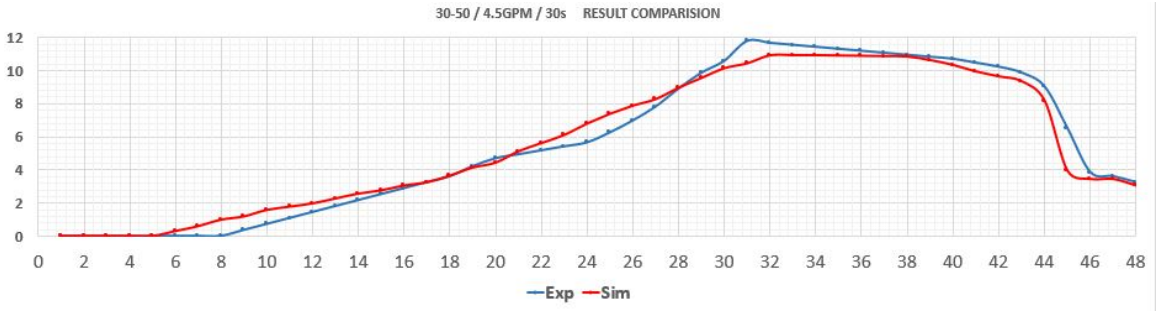


Figure 4.9: 30-50 Mesh / 4.5PPG / 30s

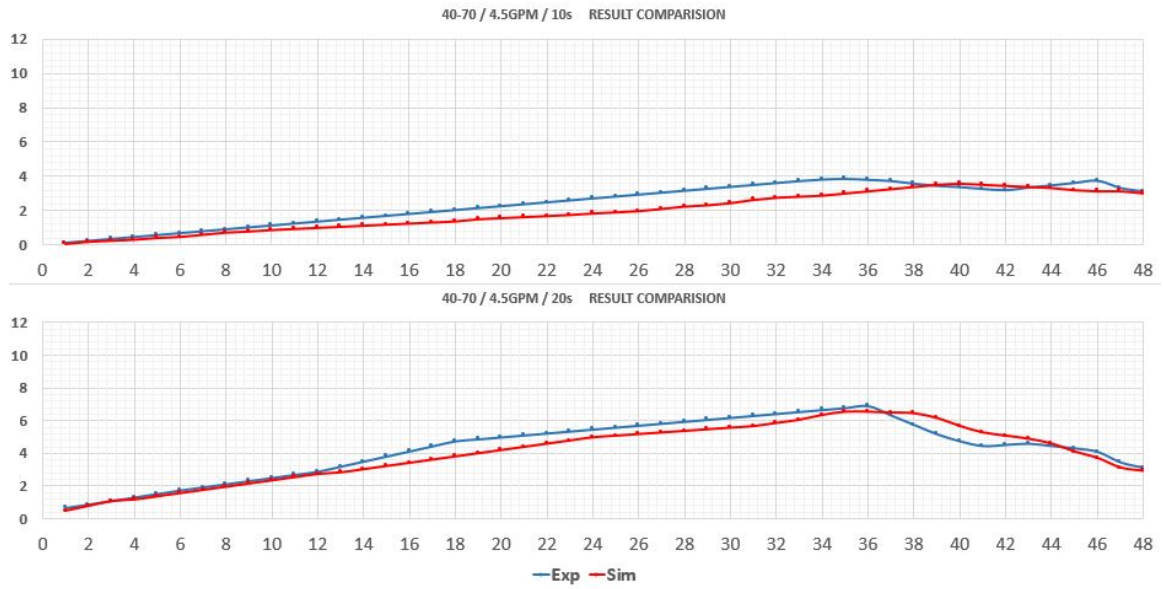


Figure 4.10: 40-70 Mesh / 4.5PPG

**Volume rate**

| **MESH** | | **20-40** | **30-50** | **40-70** |
|---|---|---|---|---|
| **GPM** | | **4.5** | **4.5** | **4.5** |
| **Time** | **10** | 109.12% | 112.36% | 123.22% |
| | **20** | 114.99% | 111.32% | 106.35% |
| | **30** | 103.82% | 100.15% | - |

**Peak Height rate**

| **MESH** | | **20-40** | **30-50** | **40-70** |
|---|---|---|---|---|
| **GPM** | | **4.5** | **4.5** | **4.5** |
| **Time** | **10** | 110.13% | 132.37% | 107.68% |
| | **20** | 130.17% | 118.22% | 105.64% |
| | **30** | 109.45% | 107.75% | - |

Table 4.1: 4.5GPM flow's volume and peak height ratio

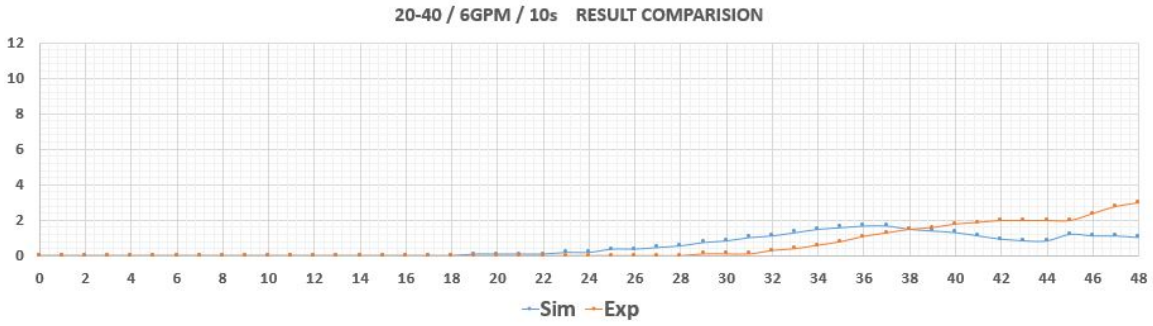


Figure 4.11: 20-40 Mesh / 6PPG / 10s

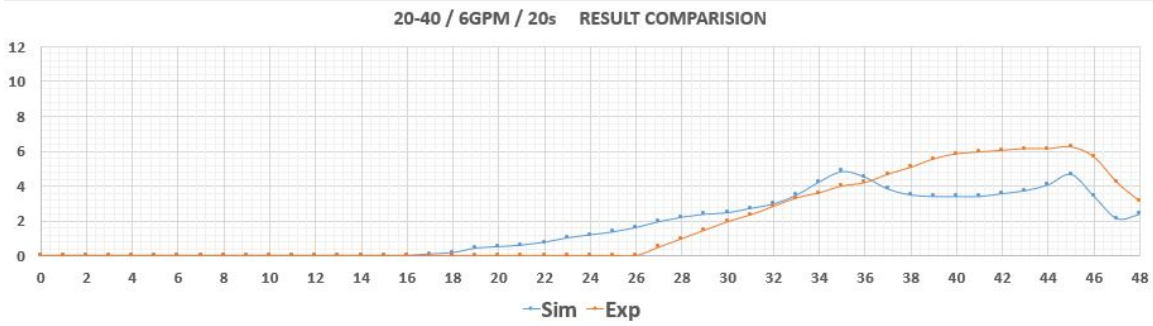


Figure 4.12: 20-40 Mesh / 6PPG / 20s

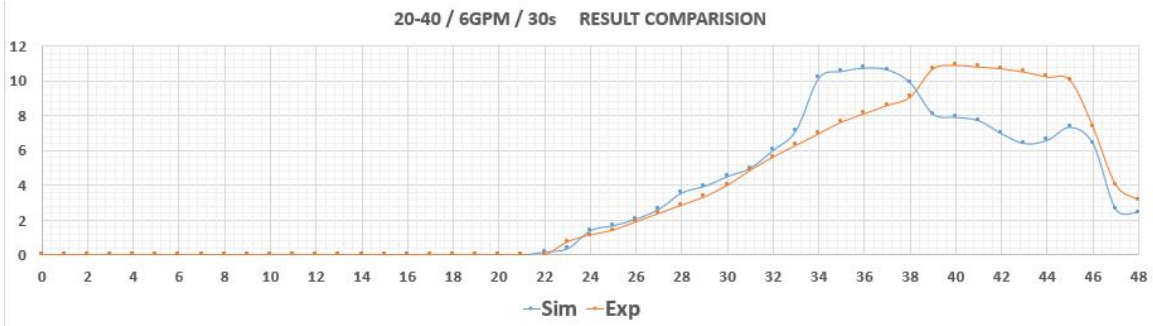


Figure 4.13: 20-40 Mesh / 6PPG / 30s

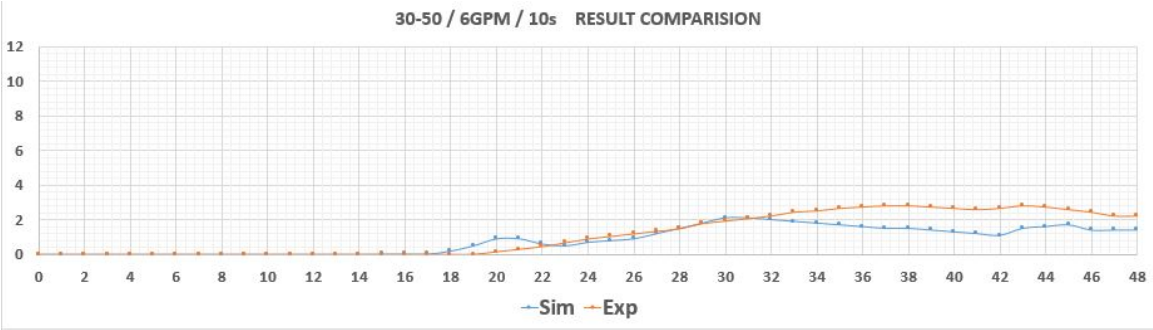


Figure 4.14: 30-50 Mesh / 6PPG / 10s

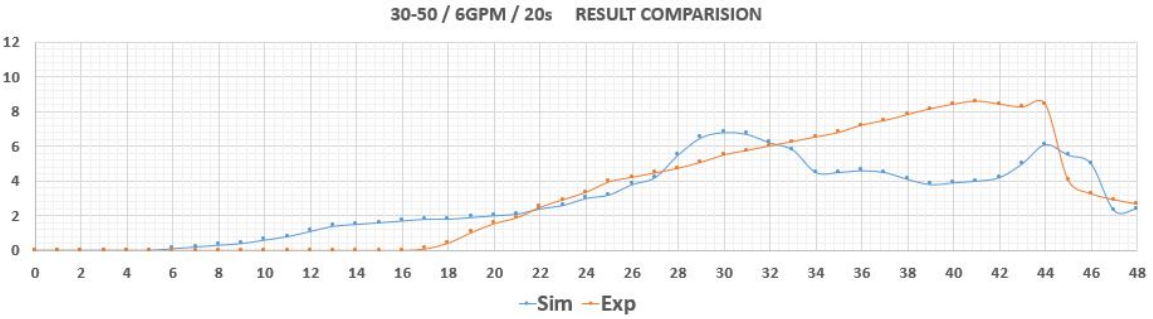


Figure 4.15: 30-50 Mesh / 6PPG / 20s

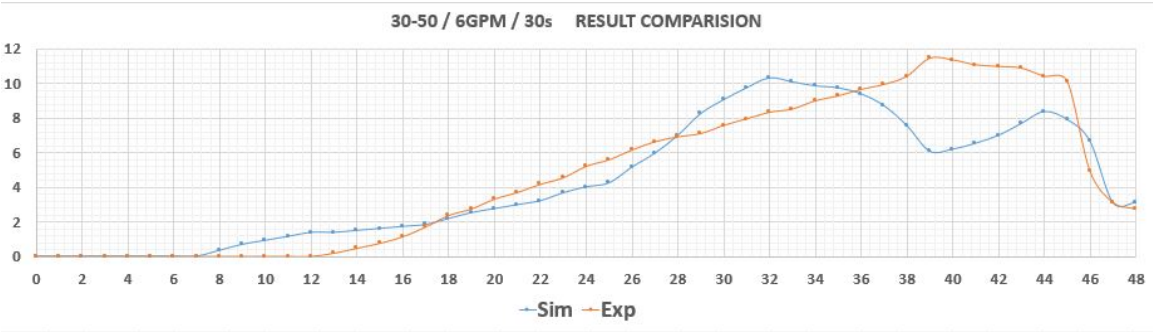


Figure 4.16: 30-50 Mesh / 6PPG / 30s

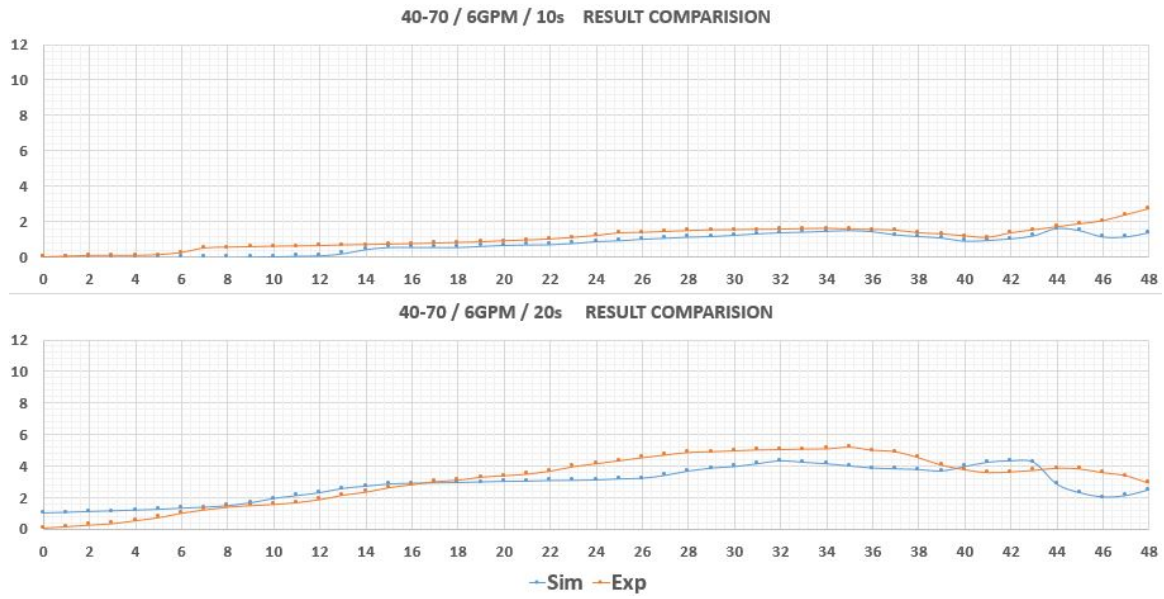


Figure 4.17: 40-70 Mesh / 6PPG

**Volume rate**

| **MESH** | | **20-40** | **30-50** | **40-70** |
|---|---|---|---|---|
| **GPM** | | **4.5** | **4.5** | **4.5** |
| **Time** | **10** | 102.21% | 142.05% | 141.28% |
| | **20** | 110.69% | 112.76% | 110.74% |
| | **30** | 106.75% | 108.96% | |

**Peak Height rate**

| **MESH** | | **20-40** | **30-50** | **40-70** |
|---|---|---|---|---|
| **GPM** | | **4.5** | **4.5** | **4.5** |
| **Time** | **10** | 173.94% | 135.69% | 168.15% |
| | **20** | 128.62% | 126.10% | 119.79% |
| | **30** | 103.55% | 111.02% | |

Table 4.2: 6GPM flow's volume and peak height ratio

## 4.2 Conclusion

The above figure 4.11 to figure 4.17 plots were obtained during the delicate investigation and simulation of this research. The height of the channel is 1 foot, and the length of the channel is 4 feet. The width of the channel is 0.5 inches. Each axis value is consistent with these relative numbers. The results of the experiment reflect the consideration that each peak point is not an exact match, because in the simulation some of forces were not considered. (e.g. turbulence deposition)

In almost all of the comparisons in these cases, there were some trend similarities and some regular gaps between each volume and peak height values. Differences are described on table 4.1 and 4.2, with volume and peak comparison ratio. However, in the consideration of each case, similar dune trends and data sets could be obtained. Still, there are many facts that should be investigated and developed, continuously.

## 4.3 Limitation of the work

There could be errors, and these are introduced in the following.

First, there could be experimental error. Fluctuations of input material occurring by agitation of the mixture, pump cavitation, and so on, could be irregular. Irregular measuring of time steps, volumes, and flowmeter data reliability can be some of the issues of experimental quantifying problem. The capturing of real time data is unavailable because of the cost, even though the results can be obtained by video hardware and image post processing. Automation of the experiment could improve the precision of the data collection process.

Secondly, the fluidized bed wasn't expressed exactly in the simulation. Also, some kind of penetration and irregular density of the dune could occur during the experiments, and it is not emphasized enough in the simulation[26]. The simulation results will be calculated by image processing. However, irregular density caused by water penetration to the sand bed cannot be discovered by computers. These kinds of volume inaccuracies are one of the reasons that the tendency of gap between experiment and simulation data exist. In almost all of the cases in this thesis, experimental data show the trend for larger time values for simulation data sets.

Thirdly, is the Angle of response. This concept is usually taken for granular materials like soil, cement, and so on. However, the considerations of under-fluidized bed conditions, should be considered, additionally. The condition of collapse is totally different under on-land conditions, and soil movement can be affected by this phenomenon. The assumption of a fully round shape particle is also one of factors for the dune formation.

Simulation errors could also be sources that contaminate results. For numerical calculations, the first order upwind scheme was taken for the reason that it was fast, efficient, and cost effective. However, every numeric value has the same problems, which are rounded off and truncated errors. Each partial differential equation definitely has similar errors because exact solutions can't be obtained[27]. That is why numerical discretization and calculations are used to get approximate solutions. Thus, the final solution data that we obtain by numerical simulations must have distortion with experimental results and real solutions.

Model selection is also one of the issues affecting the results. If the DNS model is chosen for the simulation, very fine results could be obtained, but the models require extremely high cost and time resources.

Finally, before the experiment, some of conditions should be analyzed regarding the dimensions to show matching data in real situation. In this case, the Reynold, Euler, or Froude numbers are good points to consider for the analysis. However, the experiment didn't consider sand dimension even though there are big gaps between real conditions and experimental dimensions.

### 4.4 Future work

There are many models already investigated and developed by scientists and engineers. As well, the propagation of turbulence model research is tremendously impressive, thus we can see it as a part of industrial fluid engineering. There are non-linear eddy simulation area like $\bar{v^2} - f$ models, or Large Eddy Simulation models which have possibilities that can improve abilities to obtain better results.

These sorts of endeavors are ongoing in every industry and academia, where finding appropriate automated simulation models are sought after which are adjusted to specific conditions like

complicated geometry, or micro/Nano-sized area adaptions, with some dimension scaling analysis skillsets. The Lattice-Boltzmann method is one adaptation for the microfluidics area with meshless simulation analysis[28]. Furthermore, in some parts of the turbulence modeling area, researchers have currently concentrated on figuring out an automatic coefficient solution by using multivariable regression[29].

Still, a lot of researchers are attempting to solve aforementioned problems and limitations to improve of peoples' lives. Some physical problems or model problems could be solved by appropriate assumptions and by adjusting some adequate theories. Also, some of automation problems would be solved by computing hardware environmental growth, including but not limited to, software and skillset developments. The claims for this thesis have been supported with petroleum engineering department laboratory experiments, so I hope adaption of the results will be useful for the macro petroleum area, also. Types of shale gas production improvements have already been long-ago addressed, but skills can be improved with the considerations of the limitations and endeavors that exist beyond prior limitations. With detailed parameters and detailed automated controls, probably we will obtain meaningful and impressive content.

REFERENCES


[1] S. Mimount, R. Alami, O. Hakam, A. Saadaoui, and K. El Korchi, "Development of radiometric methods for optimization of phosphate transport process by "slurry pipe"," *International Conference on Applications of Radiation Science and Technology*, vol. 1, pp. 1–29, 2017.

[2] *Collins English Dictionary*, vol. $13^{th}$ edition. HarperCollins, 2018.

[3] J. Humphrey and K. Rajagopal, "A constrained mixture model for arterial adaptations to a sustained step change in blood flow," *Biomechanics and Modeling in Mechanobiology*, vol. 2, no. 2, pp. 109–126, 2003.

[4] D. H. Beggs, J. P. Brill, *et al.*, "A study of two-phase flow in inclined pipes," *Journal of Petroleum Technology*, vol. 25, no. 05, pp. 607–617, 1973.

[5] A. Fick, "Ann," *Phys*, vol. 94, pp. 59–86, 1855.

[6] H. P. G. Darcy, *Les Fontaines publiques de la ville de Dijon. Exposition et application des principes à suivre et des formules à employer dans les questions de distribution d'eau, etc*. V. Dalamont, 1856.

[7] L. Tao and K.R.Rajagopal, *Mechanics of mixtures*, vol. 35. World scientific, 1995.

[8] K. Hutter and K. Rajagopal, "On flows of granular materials," *Continuum Mechanics and Thermodynamics*, vol. 6, no. 2, pp. 81–139, 1994.

[9] S. Subramaniam, "Lagrangian–eulerian methods for multiphase flows," *Progress in Energy and Combustion Science*, vol. 39, no. 2-3, pp. 215–245, 2013.

[10] T. N. Ofei and A. Y. Ismail, "Eulerian-eulerian simulation of particle-liquid slurry flow in horizontal pipe," *Journal of Petroleum Engineering*, vol. 2016, 2016.

[11] G. C. Howard, C. Fast, *et al.*, "Optimum fluid characteristics for fracture extension," in *Drilling and production practice*, American Petroleum Institute, 1957.

[12] T. T. Palisch, M. Vincent, P. J. Handren, *et al.*, "Slickwater fracturing: food for thought," *SPE Production & Operations*, vol. 25, no. 03, pp. 327–344, 2010.

[13] G. Johnson, M. Massoudi, and K. Rajagopal, "Flow of a fluid infused with solid particles through a pipe," *International Journal of Engineering Science*, vol. 29, no. 6, pp. 649–661, 1991.

[14] B. Van Wachem and A.-E. Almstedt, "Methods for multiphase computational fluid dynamics," *Chemical Engineering Journal*, vol. 96, no. 1-3, pp. 81–98, 2003.

[15] B. Andersson, R. Andersson, L. Håkansson, M. Mortensen, R. Sudiyo, and B. Van Wachem, *Computational fluid dynamics for engineers*. Cambridge University Press, 2011.

[16] M. Massoudi, K. Rajagopal, and T. Phuoc, "On the fully developed flow of a dense particulate mixture in a pipe," *Powder Technology*, vol. 104, no. 3, pp. 258–268, 1999.

[17] W. Rodi, *Turbulence models and their application in hydraulics*. Routledge, 2017.

[18] B. E. Launder and D. B. Spalding, "The numerical computation of turbulent flows," in *Numerical prediction of flow, heat transfer, turbulence and combustion*, pp. 96–116, Elsevier, 1983.

[19] P. Spalart and S. Allmaras, "A one-equation turbulence model for aerodynamic flows," in *30th aerospace sciences meeting and exhibit*, p. 439, 1992.

[20] J. Bredberg, "On the wall boundary condition for turbulence models," *Chalmers University of Technology, Department of Thermo and Fluid Dynamics. Internal Report 00/4. G oteborg*, 2000.

[21] W. Jones and B. E. Launder, "The prediction of laminarization with a two-equation model of turbulence," *International Journal of Heat and Mass transfer*, vol. 15, no. 2, pp. 301–314, 1972.

[22] D. Mader, *Hydraulic proppant fracturing and gravel packing*, vol. 26. Elsevier, 1989.

[23] W. C. Krumbein and L. L. Sloss, *Stratigraphy and sedimentation*, vol. 71. LWW, 1951.

[24] J. E. Bardina, P. G. Huang, and T. J. Coakley, "Turbulence modeling validation, testing, and development," 1997.

[25] D. C. Wilcox *et al.*, *Turbulence modeling for CFD*, vol. 2. DCW industries La Canada, CA, 1998.

[26] L. Huilin, H. Yurong, and D. Gidaspow, "Hydrodynamic modelling of binary mixture in a gas bubbling fluidized bed using the kinetic theory of granular flow," *Chemical Engineering Science*, vol. 58, no. 7, pp. 1197–1205, 2003.

[27] S. Patankar, *Numerical heat transfer and fluid flow*. CRC press, 1980.

[28] S. Chen and G. D. Doolen, "Lattice boltzmann method for fluid flows," *Annual review of fluid Mechanics*, vol. 30, no. 1, pp. 329–364, 1998.

[29] J. Ling, A. Kurzawski, and J. Templeton, "Reynolds averaged turbulence modelling using deep neural networks with embedded invariance," *Journal of Fluid Mechanics*, vol. 807, pp. 155–166, 2016.